Cubic optical nonlinearities with octupolar molecules at telecommunication wavelengths

G. Ramos-Ortiz, S. Romero, J.L. Maldonado, O. Barbosa-García, and M.A. Meneses-Nava
Centro de Investigaciones en Óptica,
Apartado Postal I-948, 37000 León, Guanajuato, México,
Phone: (+52 477) 441 4200, Fax: (+52 477) 441 4209,
e-mail: garamoso@cio.mx

M. Romero and N. Farfán
Departamento de Química Orgánica, Facultad de Química, UNAM,
Ciudad Universitaria, 04510 México D.F. México.

Recibido el 16 de junio de 2006; aceptado el 13 de noviembre de 2006

Here we report on the cubic nonlinear optical properties of octupolar organic molecules. A series of three compounds that were of triphenylmethane derivatives and one boroxine derivative were characterized, in solid state, at infrared wavelengths comprising telecommunication bands (900 - 1600 nm). At these wavelengths, for which there is practically an absence of reports about cubic nonlinearities in octupolar compounds, we measured third-order susceptibilities $\chi^{(3)}$ of the order of 10^{-12} esu, the latter partially enhanced by multiphoton resonances. As the molecules studied were prototypes of octupolar systems, our results correlate the magnitude of the observed nonlinearities with the molecular structure, thus providing helpful information for the design of new molecules with improved nonlinearities. On the other hand, we discuss how polymer films functionalized with these molecules can be useful for applications involving the conversion of optical frequencies. Such films produce frequency-converted signals sensitive enough that they can be employed in ultra-fast optical correlators.

Keywords: Octupolar molecules; organic materials; nonlinear materials.

Este trabajo describe las propiedades ópticas no-lineales de tercer orden de moléculas orgánicas del tipo octopolar. Una serie de tres compuestos derivados de trifenilmetano y un compuesto derivado de boroxina fueron caracterizados en estado sólido usando longitudes de onda del infrarrojo cercano, incluyendo aquellas bandas usadas en telecomunicaciones (900 - 1600 nm). Para este intervalo de longitudes de onda, para el cual prácticamente no existen reportes sobre las no-linealidades cúbicas exhibidas por moléculas octopolares, se midieron susceptibilidades no- lineales $\chi^{(3)}$ del orden de 10^{-12} esu, estas ultimas parcialmente incrementadas por resonancias multifotón. Ya que las moléculas estudiadas son prototipos de estructuras octopolares, nuestros resultados correlacionan a la magnitud de las no-linealidades observadas con la estructura molecular de forma que la información obtenida es útil para el diseño de nuevas moléculas con no-linealidades optimizadas. Por otra parte se discute el uso de películas de polímero, dopadas con dichas moléculas, en la conversión de frecuencias ópticas. Esta clase de películas producen señales ópticas convertidas en frecuencia con la sensibilidad suficiente para ser empleadas en correlacionadores ópticos de señales ultra-rápidas.

Descriptores: Moléculas octopolares; materiales orgánicos no-lineales.

PACS: 42.65.ky; 42.70.Jk; 78.20.-e

1. Introduction

Organic molecules and polymers have attracted great attention due to their optical and electro-conductive properties and because they combine low cost and ease of processing in the assembly of optical devices. In particular, these materials have potential applications in photonics as they comprise large nonlinear optical (NLO) coefficients [1, 2]. In the development of organic compounds with optimized NLO properties, most of the attention has traditionally concentrated on dipolar systems made up of electron-donor and electron-acceptor groups linked through a π-conjugated backbone (see Fig. 1a), in which the NLO response is due to a unidirectional charge excitation. More recently, however, optical nonlinearities have been observed in molecules with higher polar contributions, *i.e.*, quadropolar or octupolar [3, 4]. In the latter case, for example, a symmetrical arrangement of donor/acceptor substituents (see Figs. 1b and 1c) cancel the dipole moment in the molecule (in both the ground state and excited state) while the NLO response occurs upon photoexcitation due to octupolar contributions deriving from charge transfer along three different axes [4]. Thus, the increasing interest for studying materials with octupolar structure arises from a basic science perspective which seeks to understand the multipolar contribution to nonlinearities, but has also been motivated by practical reasons since such systems could overcome some drawbacks present in macroscopic assemblies based on dipolar units: the tendency to aggregation in solid state and the NLO efficiency/transparency tradeoff always present in organics. Some representative reports on the theoretical and experimental studies of nonlinearities in octupolar systems are found in Refs. 4 to 7.

It should be observed that very few reports exist on the third-order NLO properties of octupolar molecules, as they were originally conceived for quadratic NLO effects, in fact, it was not until recently that the multidirectional charge trans-

fer occurring in octupolar compounds was correlated with third-order NLO effects; such as two-photon absorption and an intensity-dependent refractive index for the wavelength range of 500 - 800 nm [8–11]. In order to get a better insight into the potentiality of octupolar systems, in this work we present the characterization of the cubic NLO properties of some of these compounds over the wavelength range of 900 - 1600 nm, which is of interest for applications to telecommunications.

For the present work we used the compounds whose molecular structures are shown in Fig. 2. The molecules BF (Basic Fuchsin), CV (Crystal Violet) and MG (Malachite Green) are derivatives of triphenylmethane and are well-known dyes used traditionally as histological stains or as PH indicators [12]. BF and CV were chosen for this study because they can be considered a series of donor-substituted prototypes of the octupolar structure shown in Fig. 1c), while MG was included because it has a quasi three-fold symmetry (*i.e.* its character is not entirely octupolar), so that we can find the effect of the molecular symmetry on the cubic NLO properties by comparing MG with BS and CV. Finally, the fourth molecule, denoted as BO in Fig. 2, is a boroxine derivative possessing the octupolar structure (shown in Fig. 1c). This boroxine is of interest to us because it provides a route for the design of octupolar molecules with high optical transparency.

For the nonlinear optical characterization, we utilized the third-harmonic generation (THG) process exhibited by the octupolar molecules. The choice of measuring nonlinearities of the type $\chi^{(3)}(-3\omega;\omega,\omega,\omega)$ is partly because it allowed us to know the magnitude of pure electronic NLO effects (important for photonic applications such as high bandwidth all-optical switching), but was also motivated by our intention to evaluate the THG performance, as a bulk effect, in polymer films functionalized with octupolar dyes. Recent reports have demonstrated the utility of organic thin films applied to ballistic photon imaging through non-collinear THG [13] and ultrafast pulse diagnosis with THG autocorrelation [14, 15].

2. Sample preparation and characterization of their linear optical constants

The triphenylmethane derivatives CV and BF were acquired as chloride salts and MG as an oxalate salt from the company Sigma-Aldrich. The compounds were processed as received with purities > 90 %. On the other hand, the boroxine derivative BO was synthesized in our labs according to routes reported elsewhere [16,17]. The molecules were studied in solid state (solid films) using the guest(molecule)-host(polymer) approach. By using the polymer PMMA as a host, we prepared composites with a nonlinear material loading of 30 wt.% (weight percent). The high solubility of the composites in a variety of solvents made it possible to obtain homogeneous films of good optical quality that were deposited on fused silica substrates (1 mm-thick) by using the spin-coating technique. Film thickness was controlled with the rotation speed of our spin-coater and with the viscosity of solutions, so that thicknesses of between 0.05 μm and 10 μm were obtained. These thicknesses were measured with an AFM (Atomic Force Microscope) for thicknesses < 1 μm, while thicker films were measured with a thin-film measurement system (Filmetrics F20). The absorption spectra of spin-coated films were measured with a spectrophotometer (Perkin-Elmer Lambda 900) and their refractive index dispersion curves were calculated from the absorption spectra by using the Kramers-Kronig transformations. To match the dispersion curves to the correct refractive index values, we measured the refractive index at 700 nm from the films' interference reflection spectra using the Filmetrics F20 system.

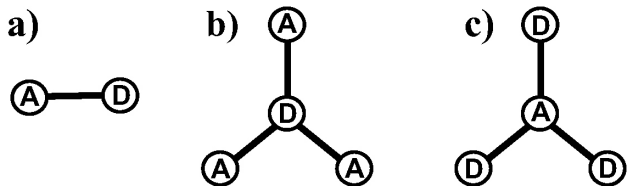

FIGURE 1. Diagram of nonlinear organic molecules characterized by different dimensionality: a) dipolar; b) and c) octupolar. D and A denote electron donor/acceptor groups, respectively. The lines connecting D and A depict π-conjugated bridges comprising a chain of bonded carbon atoms with alternate single and double covalent bonds.

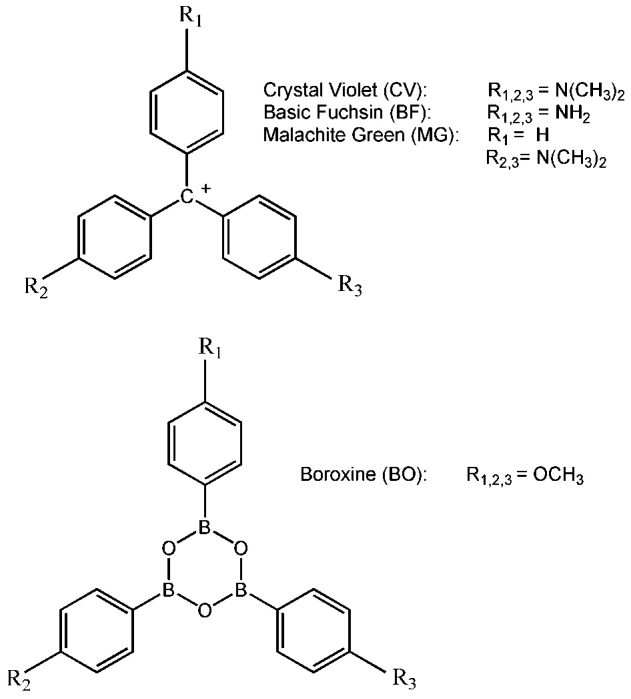

FIGURE 2. Chemical structure of the triphenylmethane dyes Basic Fuchsin (BF), Crystal Violet (CV), Malachite Green (MG) and the boroxine derivative BO. R_1 and R_2 denote donor-substituent groups.

3. Experimental setup to measure $\chi^{(3)}$ in samples

To measure THG from our samples, we used as pump source a Nd-YAG laser-pumped optical parametric oscillator (OPO) that delivered pulses of 8 ns at a repetition rate of 10 Hz. The idler beam of the OPO system was focused onto the films with a 30-cm focal-length lens to form a spot with a radius of approximately 150 μm. For our purposes the idler wavelength was tuned within the range 900 - 1600 nm, and to avoid degradation the energy per pulse at sample position in any case was set to less than 2 mJ (corresponding to peak intensities of 0.35 GW/cm^2). The third-harmonic beam emerging from the films was separated from the pump beam by using a color filter and detected with a system made up of a monochromator, photomultiplier tube (PMT) and a Lock-in amplifier. The THG signals thus obtained were calibrated to take into account the energy fluctuations of the pump beam, the PMT sensibility, and the transmission of the color filter as a function of the wavelength.

4. Basic theory of third-harmonic generation in films

To make the characterization of the third-order nonlinearities in our samples by means of THG-signal analysis, we derived simple expressions valid in the plane-wave approximation. By following the same procedure used in text books [18] to solve the wave equation in the case of second-harmonic signals (assuming negligible power depletion in the pump beam E_ω), it is straightforward to demonstrate that the third-harmonic electric field $E_{3\omega}$, generated from a film of thickness L, can be written as:

$$E_{3\omega} = \frac{1}{4}\chi^3 \Gamma E_\omega^3 \tag{1}$$

with

$$\Gamma = \left[\left(\frac{6\pi}{\lambda}\right)^2 \frac{1-\exp(-i\Delta kL)}{k_{3\omega}^2 - (3k_\omega)^2},\right] \tag{2}$$

where $\chi^{(3)}$ is the third-order nonlinear susceptibility of the film, λ the fundamental wavelength, while k_ω and $k_{3\omega}$ are the wavevectors for the fundamental and third harmonic, respectively. Here, we consider the THG process in a collinear geometry, so the wavevector mismatch between the co-propagating waves is a scalar quantity denoted by $\Delta k (\equiv k_{3\omega} - 3k_\omega)$.

According to Eq. (1), the THG output depends not only on $\chi^{(3)}$ and the amplitude of the electric field in the fundamental wave, but also on the linear optical constants that characterize the films at both the fundamental and the third harmonic wavelengths. In order to use Eq. (1) to calculate $\chi^{(3)}$, we first need to know the values of all the linear optical constants enclosed in the bracket that appears in the right-hand side of Eq. (2). In addition, we can consider a reference sample (fused silica in our experiments) for which the values of $\chi^{(3)}$ and the linear constants are well characterized. Therefore, by testing our organic films and the reference sample under the same experimental conditions, and by comparing their THG signal intensities, we deduce from Eq. (1) that the unknown third-order nonlinear susceptibility is given by:

$$|\chi^{(3)}|_{film} = |\chi^{(3)}|_{ref} \frac{|\Gamma|_{ref}}{|\Gamma|_{film}} \left(\frac{[I_{3\omega}]_{film}}{[I_{3\omega}]_{ref}}\right)^{1/2}, \tag{3}$$

where $I_{3\omega}$ denotes the THG intensities detected experimentally.

5. Experimental results and discussion

5.1. Measurement of linear optical constants in polymer films doped with octupolar molecules

Figure 3 shows the linear absorption spectra and the corresponding real part of the refractive index for polymer films doped with BF, CV and MG. Here we see that these dyes have a main absorption peak at 550, 540 and 660 nm, respectively, with windows of relative minimum absorption between 330 and 500 nm and almost null absorption for wavelengths longer than 800 nm. In Fig. 3 we omitted the absorption curve of the octupolar molecule BO, since it only has a principal absorption peak at 270 nm and is optically transparent beyond 325 nm. Due to the absorption bands that BF, CV and MG exhibit in the UV-VIS range of the spectrum, the refractive indexes of the films were actually given by complex numbers and so the wavevectors k_ω and $k_{3\omega}$ also resulted in complex expressions (recall that $k_\omega = (\omega/c)n_\omega$ and $k_{3\omega} = (3\omega/c)n_{3\omega}$). To calculate the imaginary part of k_ω and $k_{3\omega}$, we followed the convention that this imaginary term is related to the absorption coefficient α by $Im\{k\} = \alpha/2$. So, once α was measured in the films, we employed an algorithm based on Kramers-Kronig relations to calculate the real part of the refractive index following the procedure mentioned in Sec. 2, and in that way the wavevectors were fully characterized.

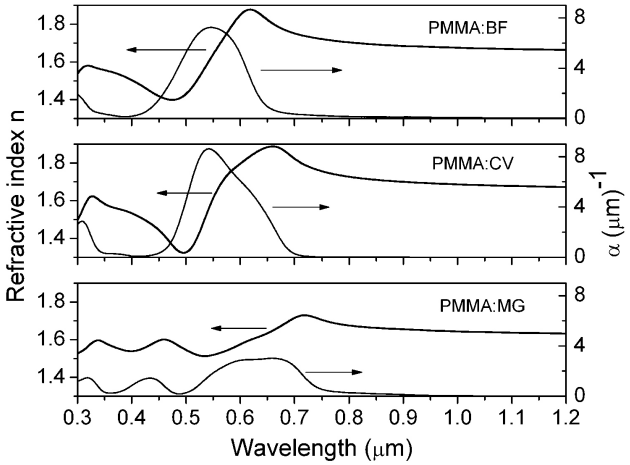

FIGURE 3. Refractive index dispersion and absorption coefficient of PMMA films doped with 30 wt.% of the BF, CV and MG dyes, respectively.

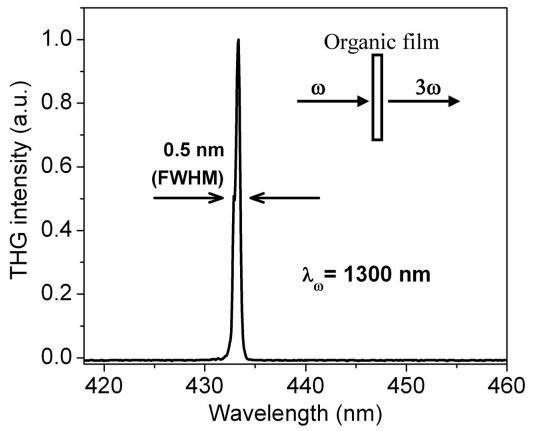

FIGURE 4. Normalized THG spectrum measured at a fundamental wavelength of 1300 nm. This spectrum was always the same independently of the nonlinear molecule used to measure it.

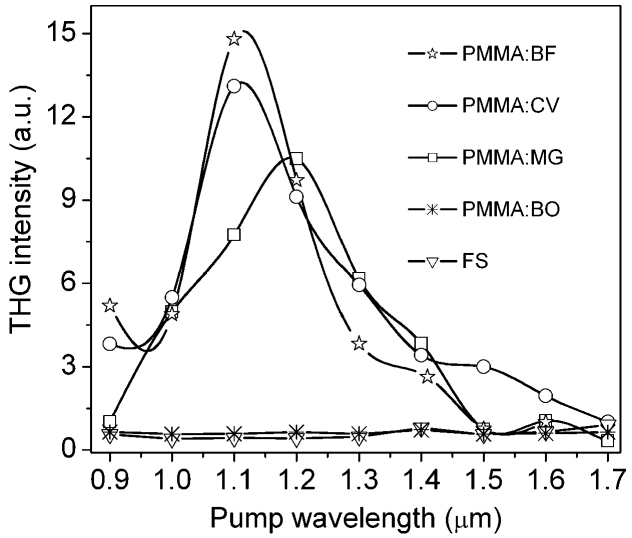

FIGURE 5. THG intensity versus fundamental wavelength measured in PMMA films doped with 30 wt.% of BF, CV, MG and BO. The film thicknesses are 6.8, 5, 2.5 μm and 0.5 μm, respectively. FS denotes a 1 mm-thick fused silica glass slab. All data are calibrated with respect to changes in pump power at different wavelengths and the continuous lines are guides for the eye.

5.2. THG spectra and calculation of third-order nonlinear susceptibilities in polymer films doped with octupolar molecules

After the characterization of the linear optical constants was performed, we proceeded to quantify the magnitude of the nonlinear susceptibility $\chi^{(3)}$ in the polymer-dye composites. In our experiments, a beam of THG generated in such composites was easily detected; as an example of this, Fig. 4 presents the THG spectrum corresponding to a fundamental wavelength of 1300 nm (note that the measured bandwidth in this THG spectrum was only limited by the resolution of the detection system). We remark that the THG signal at any specific pump wavelength was always characterized by this kind of very sharp peak, as should occur according to the pump bandwidth ($<$0.01 nm). Moreover, the normalized THG spectrum was always the same independently of the nonlinear molecule used to measure it. On the other hand, Fig. 5 presents the maximum values of the THG peaks exhibited by the films at different pump wavelengths (the data are calibrated with respect to changes in pump power at different wavelengths); here it is observed that those films doped with BF, CV and MG had significant THG production in broad-bands of pump wavelengths of approximately 200 nm (FWHM) centered at 1110 nm, 1115 and 1190 nm, respectively. In the case of the octupolar BO, however, the THG signal was practically a constant for the entire range of pump wavelengths. Figure 5 also includes the THG signals detected in a 1 mm-thick fused silica glass slab used as reference material. Therefore, by comparing the THG signals from the films tested with those from the reference glass through the method explained in Sec. 4, and by using the optical constants already measured for the films, we were able to obtain the $\chi^{(3)}_{film}$ values. To perform these calculations, we plugged into Eq. (3) tabulated refractive index values available for fused silica [19] and considered that $\chi^{(3)}_{film} = 3.1 \times 10^{-14}$ esu (which is practically a constant for the range of wavelengths used in our experiments [20]).

Figure 6 presents the nonlinearity dispersion for the case of BF, CV and MG, showing typical values of the order of $\chi^{(3)}_{film} \approx 10^{-12}$ esu. To understand what is at the origin of the dispersion in the $\chi^{(3)}_{film}$ values shown in Fig. 6, we refer to the resonance features that result from the molecular electronic properties. Two-photon and three-photon resonances can enhance $\chi^{(3)}$ significantly when the energy difference between transition-allowed electronic levels are close to 2 or $3\hbar\omega$, with ω being the excitation wavelength. To see this, in Fig. 6 we included the electronic transitions (the linear absorption spectra) of each molecule with the wavelength multiplied by a factor of two and three, respectively. Although in this figure we clearly see the multiphoton resonance enhancement of $\chi^{(3)}_{film}$, it is not totally understood whether it corresponds to two or three photons or a combination of both. A better insight into resonance features would imply theoretical calculations of excited state parameters based on the molecular structure and extend the wavelength range in our measurements. In regard to BO, we obtain $\chi^{(3)}_{film} \approx 10^{-14}$ esu with practically null dispersion (not shown in the figure) due to the absence of such resonances.

As for the maximum magnitude of $\chi^{(3)}_{film}$ obtained for each molecule, our experiments clearly reveal the role played by the electron-donor substituent groups. For instance, it is well known that the donating strength of the dimethylamine substituent ($N[CH_3]_2$) is more effective than that of the amine substituent (NH_2) [21]; as a consequence, there was a stronger intramolecular charge transfer in CV with respect to BF, which results in larger values of $\chi^{(3)}$ in the first

case (see Fig. 6). Likewise, the role played by the molecular symmetry is clearly evident by contrasting MG and CV (both having $N[CH_3]_2$ as donor groups); in MG the reduced dimensionality (lack of symmetry) implied a weaker charge transfer from the periphery to the core of the molecule, so a pronounced reduction of nonlinearity was observed. It is also worth comparing the maximum values of $\chi^{(3)}$ measured for these triphenylmethane dyes with the only report existing for other octupolar molecules in the same wavelength range. For example, Park *et al*. [22] measured a value of 1.2×10^{-11} esu for the octupolar molecule TTB in solid state in experiments performed at 1064 nm. Although we measured smaller nonlinear susceptibilities in BF, CV and MG, it is important to point out that the NLO properties in these dyes are not tailored, as their original chemical design (made decades ago) was aimed at industrial purposes other than NLO processes [12]. For this reason, we believe that the nonlinear optimization of compounds based on triphenylmethane dyes is still feasible by incrementing the π-conjugation (number of single and double covalent bonds in the molecule branches) and by using more effective electron-donor substituents. These conditions favor a stronger charge transfer and in turn would enhance the molecular nonlinearities. With regard to the octupolar BO, we had mentioned that the lack of resonance translated into a weak nonlinearity. Despite this result, we think that it is important to continue evaluating such structures, since the introduction of a boroxine core could provide an innovative route for the optimization of cubic NLO effect with a good nonlinearity-transparency trade-off, as was demonstrated for the case of quadratic nonlinearities [16]. In very recent times, new designs of this kind of boroxines have been reported [23].

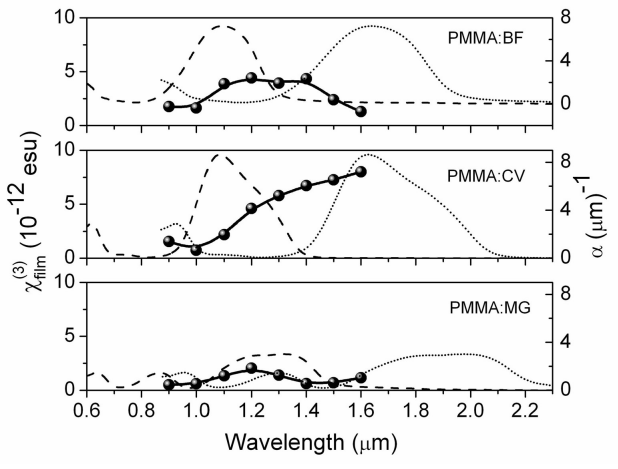

FIGURE 6. Third-order nonlinear susceptibility dispersion for polymer films doped with 30 wt.% of BF, CV and MG, respectively. The continuous lines are guides for the eye. As reference for multiphoton resonances, the dashed and dotted lines describe the electronic allowed transitions (absorption spectrum) of each dye with the wavelength multiplied by a factor of two and three, respectively.

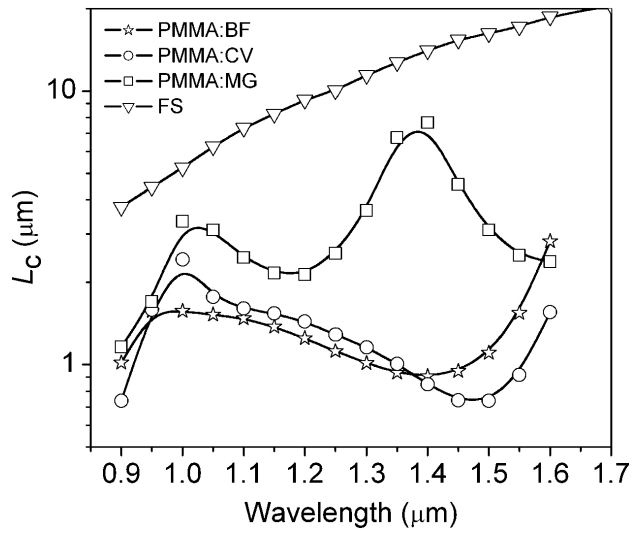

FIGURE 7. Coherence length calculated for the polymer films doped with 30wt.% of BF, CV and MG, respectively, and for fused silica (FS) substrate. The continuous lines are guides for the eye.

Finally, we mention that due to limitation in our detection systems at UV wavelengths, we could not extend the THG experiments for fundamental wavelengths shorter than 900 nm; this precluded the measurement of cubic nonlinearities in the vicinity of the main absorption bands. Nevertheless, for CV and BF an increase in the THG signal was clearly observed as our OPO system was tuned from 1000 to 900 nm (see Fig. 5). This result suggests that in these molecules there exists another band with maximum values of $\chi^{(3)}_{film}$ (different from those shown in Fig. 6) for wavelengths shorter than 900 nm. This suggestion is in agreement with the existence of a two-photon absorption band predicted theoretically and detected experimentally between 700 and 800 nm for the CV molecule due to $S_1 \rightarrow S_0$ and $S_2 \rightarrow S_0$ transitions [9, 10, 24]. We point out that the authors of Ref. 10 detected almost null nonlinear absorption for wavelengths longer than 900 nm, so by comparing their results and ours we can infer that, in the case of CV, the susceptibility $\chi^{(3)}$ might have a significant imaginary component for $\lambda < 1000$ nm and a small imaginary component for $\lambda > 1000$ nm. Due to their structural similarities, the same reasoning might apply to BF.

5.3. Frequency-converted signals as a bulk effect in thick polymer films functionalized with octupolar dyes

As the THG signals detected in our experiments originated from a bulk effect, the film optical constants played an important role in the experiment sensitivity. For example, the index dispersion determined the level of phase mismatch Δk between the fundamental and harmonic waves, so that the interaction length for which there was an effective accumulation of THG along the sample thickness was limited by the coherence length $L_c = \pi/\Delta k$ [18]. Figure 7 presents the coherence lengths of our composites calculated from the corresponding refractive index dispersion curves (see Fig. 3). We

see that in a THG collinear geometry these coherence lengths are rather small and shorter than the thickness of our films, but it should be noticed that in a noncollinear geometry they can be increased notably (see discussion below). Similarly, the absorption set another limit to THG (in Fig. 5 the wavelength dependence of the THG intensity was strongly correlated to the absorption spectra).

Although here we have used the detection of THG signals as a method to calculate the magnitude of nonlinearities in octupolar compounds, generally the creation of THG directly from the third-order nonlinearity is of little practical importance because of the small value of $\chi^{(3)}$ and the strong refractive index dispersion of most materials. As a matter of fact, except for the THG-microscopy, the use of THG has only found wide application in the measurement of cubic nonlinearities in organics through the Maker-Fringes method [2, 20]. Although the latter is a powerful technique for determining the magnitude and phase of $\chi^{(3)}_{film}$, it implies knowing accurately the contributions to the THG signals originated at the air-film and air-substrate interfaces, and for that reason most authors use a simplified version of this technique to quickly screen the magnitude of $\chi^{(3)}_{film}$ (though tolerating certain uncertainty in its absolute value). This simplification uses very straightforward equations and eliminates the need for the fitting procedure of THG-fringes, so that the magnitude of $\chi^{(3)}_{film}$ is estimated by simply comparing the THG peaks produced from films (much thinner than L_c) deposited on a reference substrate to the ones produce by the substraed alone. In our case, however, we followed a different approach in measuring the magnitude of $\chi^{(3)}_{film}$ and in studying the THG as a bulk effect in thick films (we estimate that the errors in measuring $\chi^{(3)}_{film}$ with our experimental approach should be similar to those generated by the simplified version of the Maker-Fringes). Thus, even though the bulk effect in our experiments was limited to a few microns through L_c, robust THG signals were produced as a consequence of an intermediate $\chi^{(3)}_{film}$ value, small absorption at some harmonic wavelengths, and by the high optical quality of the films. On the other hand, those films doped with the octupolar dyes CV, BF and MG have the property of being negatively dispersive materials (see Fig. 3) which is very advantageous for the implementation of near phase-matched THG process in a noncollinear geometry (in these geometries it is possible to increase substantially the L_c values shown in Fig. 7), as was demonstrated for applications involving optical correlation generated in films made of the conducting polymer PPV and polymer films doped with dipolar molecules [13–15]. Our claim is that in addition to these applications, the octupolar compounds can also be useful in implementing a third-order SFG (*Sum Frequency Generation*) process where two different wavelengths pump an organic film. This NLO process can have implications in telecommunication applications such as *optical sampling* where one optical signal (*i.e.* 1500 nm) is monitored by a reference signal (*i.e.* 1064 nm) through the correlation of both in a nonlinear medium to produce SFG [25]. In our laboratories, we are currently implementing experiments in this direction.

6. Conclusions

In summary, we characterized the cubic susceptibility of octupolar molecules in the wavelength range 900 - 1600 nm where we measured $\chi^{(3)} \approx 10^{-12}$ for triphenylmethane derivatives and $\chi^{(3)} \approx 10^{-13}$ for a boroxine derivative, all in solid state. The implications of the substitution of donor-groups and molecular symmetry on the magnitude of $\chi^{(3)}$ were examined, confirming that, as in the case of dipolar structures, in octupolar molecules the cubic NLO effects can be optimized with a large enough conjugation along the molecular backbone and strong donator/acceptor groups. Based on the octupolar prototypes studied here, new molecules with improved nonlinearities can be tailored. On the other hand, polymer-octupolar dye composites were easy to process, and offer the possibility of integration into films to frequency-convert fundamental wavelengths within the range of telecommunications. We remark that, despite the small efficiencies attainable in the conversion of IR frequencies with the use of organic films, the latter offer low-cost solutions for ultra-fast optical correlators.

Acknowledgments

The authors wish to thank Dr. Sergio Calixto for the film thickness measurements with AFM and Dr. Raúl Vázquez-Nava for processing the manuscript in LaTeX. This work was supported by CONCyTEG (Project 05-04-K117-026 A02) and by CONACyT (Project J40775-F).

1. P.N. Prasad and D.J. Williams, *Introduction to nonlinear optical effects in molecules and polymers* (John & Wiley, New York 1991).
2. M.G. Kuzyk and C.W. Dirk, *Characterization techniques and tabulations for organic nonlinear optical materials* (Marcel Dekker, New York, 1998).
3. L. Ventelon, L. Moreaux, J. Mertz, and M. Blanchard-Desce, *Synthetic Metals* **127** (2002) 17.
4. J. Zyss and I. Ledoux, *Chem. Rev.* **94** (1994) 77.
5. T. Verbiest, S. Houbrechts, M. Kauranen, K. Clays, and A. Persoons, *J. Mater. Chem.* **7** (1997) 2175.
6. Y.K. Lee, S.J. Jeon, and M. Cho, *J. Am. Chem. Soc.* **120** (1998) 10921.
7. W. Zhu and G.S. Wu, *J. Phys. Chem. A* **105** (2001) 9568.
8. B. Derkowska *et al.*, *J. Opt. Soc. Am. B* **18** (2001) 610.

9. W. H Lee *et al., J. Am. Chem. Soc.* **123** (2001) 10658.
10. D. Beljonne *et al., Advanced Functional Materials* **12** (2002) 631.
11. X. Zhou, J.K. Feng, and A.M. Ren, *Chem. Phys. Lett.* **403** (2005) 7.
12. Klau Hunger, Ed., Industrial Dyes. Chemistry, Properties and applications. Wiley-Vch., Germany 2003.
13. G. Ramos-Ortiz *et al., Opt. Lett.* **29** (2004) 2515.
14. M. Samoc, A, Samoc, and B. Luther-Davies, *Opt. Exp.* **11** (2003) 1787.
15. G. Ramos-Ortiz *et al., App. Phys. Lett.* **85** (2004) 3348.
16. G. Alcaraz *et al., Chem. Commun.* **22** (2003) 2766.
17. Y. Tokunaga, H. Ueno, Y. Shimomura, and T. Seo, *Heterocycles* **57** (2002) 787.
18. See, for instance, R.W. Boyd, *Nonlinear Optics* (Academic Press, San Diego USA, 1992).
19. Melles-Griot, *Optics Guide*, http://www.melles-griot.com.
20. F. Kajzar and J. Messier, *Phys. Rev. A* **32** (1985) 2352.
21. See, for instance, M.C. Gupta, *Handbook of photonics* (CRC Press, USA, 1997).
22. J.H. Park, M. Cha, M.Y. Jeong, and B.R. Cho, *J. Korean Phys. Soc.* **45** (2004) 371.
23. E.K. Perttu, M. Arnold, and P.M. Iovine, *Tetrahedron Letters* **46** (2005) 8753.
24. Y. Rao, X.M. Guo, Y.S. Tao, and H.F. Wang, *J. Phys. Chem. A* **108** (2004) 7977.
25. H. Ohta, N. Yamada, N. Nogiwa, and Y. Yanagisawa, *Electron. Lett.* **37** (2001) 1541.